Molecular Crystals and Liquid Crystals

ISSN: 1542-1406 (Print) 1563-5287 (Online) Journal homepage: http://www.tandfonline.com/loi/gmcl20

Effect of Laser Fluence on the Characteristics of ZnO Nanoparticles Produced by Laser Ablation in Acetone

Davoud Dorranian & Atefeh Fotovat Eskandari

To cite this article: Davoud Dorranian & Atefeh Fotovat Eskandari (2015) Effect of Laser Fluence on the Characteristics of ZnO Nanoparticles Produced by Laser Ablation in Acetone, Molecular Crystals and Liquid Crystals, 607:1, 1-12, DOI: 10.1080/15421406.2014.927414

To link to this article: http://dx.doi.org/10.1080/15421406.2014.927414

Published online: 26 Feb 2015.

Submit your article to this journal

Article views: 41

View related articles

View Crossmark data

Full Terms & Conditions of access and use can be found at
http://www.tandfonline.com/action/journalInformation?journalCode=gmcl20

Download by: [University Town Library of Shenzhen] **Date:** 02 January 2016, At: 04:10

Mol. Cryst. Liq. Cryst., Vol. 607: pp. 1–12, 2015
Copyright © Taylor & Francis Group, LLC
ISSN: 1542-1406 print/1563-5287 online
DOI: 10.1080/15421406.2014.927414

Taylor & Francis
Taylor & Francis Group

Effect of Laser Fluence on the Characteristics of ZnO Nanoparticles Produced by Laser Ablation in Acetone

DAVOUD DORRANIAN* AND ATEFEH FOTOVAT ESKANDARI

Laser Lab., Plasma Physics Research Center, Science and Research Branch, Islamic Azad University, Tehran, Iran

We have studied the effects of the laser fluence on the characteristics of ZnO nanoparticles produced by pulsed laser ablation (PLA) of Zn plate in acetone. The beam of a Q-switched Nd:YAG laser of 1064 wavelength at 7 ns pulse width and different fluencies was employed to produce nanoparticles. The ZnO nanoparticles were found to be hexagonal. The size distribution of generated nanoparticles is increased by increasing the laser fluence. The production rate of nanoparticles is increased with increasing the laser fluence. ZnO nanoparticles were formed with spherical shape. The bandgap energy of nanoparticles is calculated to be 3.59–3.89 eV. In this range of ZnO nanoparticle size, photoluminescence spectrum exhibits two peaks due to bandgap transition and defect levels.

Keywords Nanoparticle; photoluminescence; pulsed laser ablation; SEM; size distribution; TEM; zinc oxide

Downloaded by [University Town Library of Shenzhen] at 04:10 02 January 2016

1. Introduction

There is a growing interest in the fabrication of nanomaterials and their applications in various fields of life and technology such as electronics, health care, energy generation, and storage. Nanoparticles are at the focus of scientific investigations for many technological applications and fundamental research due to their size-dependent physical properties [1]. Properties of material are known to be strongly dependent on the chemical nature and the structure of its constituents, in particular, due to overlapping their atomic or molecular orbitals. Bulk materials composed of a large number of atoms, are characterized by the presence of energy bands, which are responsible for most of physical and chemical properties of solids. However, for nanomaterials with dimension between few to 100 nm, the number of atoms becomes so small that the electronic energy bands are significantly modified, strongly affecting almost all physical properties of the materials [2]. Those significant properties, such as chemical, electronic, mechanical, and optical properties, of nanoparticles obviously distinguish them from those of the corresponding "bulk" material.

*Address correspondence to Davoud Dorranian, Laser Lab., Plasma Physics Research Center, Science and Research Branch, Islamic Azad University, Tehran, Iran. Tel.: +98 21 44869 654; Fax: +98 21 44869640. E-mail: doran@srbiau.ac.ir

Color versions of one or more of the figures in the article can be found online at www.tandfonline.com/gmcl.

Downloaded by [University Town Library of Shenzhen] at 04:10 02 January 2016

Among different nanoparticles ZnO has attracted great interests because of its several interesting applications in different fields. ZnO is a compound chemically and thermally stable n-type semiconductor which is distinguished for its wide direct bandgap (3.37 eV) [3]. The nanostructure of ZnO is the key component of photonic devices, sensor array, and catalyst because of this wide direct bandgap, as well as its high exciton binding energy at room temperature (60 meV) [4, 5]. The best advantage of ZnO is its low price, good gas-sensing properties, photocatalytic activity, and antibacterial activity. This semiconductor nanoparticle shows possibility to prepare structures with interesting optical properties such as photonic crystals. In small amount, ZnO is not toxic. Additional advantage of ZnO is that it can be easily processed by wet chemical etching and that it has excellent stability under high-energy radiation [6, 7].

A wide variety of techniques have been exploited to fabricate ZnO nanostructures. Most well-defined ZnO nanostructures with an abundant variety of shapes, such as nanorods, nanoneedles, nanotubes, nanobelts, flower-, spindle-, tower-like structures have been synthesized by traditional methods based on the high-temperature vapor-based techniques or the chemical solution route [8]. Among others, the pulsed laser ablation (PLA) method has been attracting much interest for producing organic nanoparticles and is better suited for organic compounds that are nonwater-soluble or water-soluble resistant [9]. The important features of PLA technique are that one can prepare well-crystallized nanoparticles which are pure without by-products [10]. PLA technique for synthesis of nanostructured materials from a solid target in liquid media has many advantages. The first advantage of the PLA technique is inexpensive equipment for controlling the ablation atmosphere. Most importantly, it has been demonstrated that size of synthesized material can be controlled by changing different parameters such as laser wavelength, pulse laser duration, changing the PH of the solution, adding surfactants, and changing the temperature of solution [11, 12].

Producing ZnO nanoparticles by laser ablation in different aqueous media has been reported by He et al. [13]. They employed a nanosecond UV laser pulse to generate ZnO nanoparticles. In their experimental condition, the lattice of generated nanoparticles in different solvent was not changed. Sizes of produced nanoparticles were in the range of 10–35 nm. In another report by He et al., the production of ZnO nanoparticles in CTAB and deionized water was published [14]. The same laser was employed. They observed that the morphology of nanoparticles strongly depends on the solution material. Rate of ablation in CTAB is larger than other environments. Faramarzi et al. investigated the effect of polymeric materials in the ablation medium [15]. The average particle diameters of nanocomposites which was produced by 75 μJ pulse energy in the liquid with 0.4 Wt% polymer concentration were in the range of 0.5–16 nm. The typical size of nanocomposites was decreased from 8 nm to 6 nm by 0.1 Wt% increasing in polymer concentration. They showed the possibility of production of $<$10 nm size ZnO nanoparticles with picosecond pulsed laser of 515 nm wavelength.

In this manuscript, we have investigated the effect of laser pulse energy on the characteristics of ZnO nanoparticles produced by laser ablation of a Zn bulk in acetone. Effect of laser pulse energy on the size distribution as well as lattice structure and morphology of nanoparticles are studied experimentally.

2. Experimental Set Up

ZnO nanoparticles were produced by pulse laser ablation of a Zn plate (99.99%) placed at the bottom of a glass vessel filled with 5 mL acetone (from Merck Co.) at 12 mm

Table 1. Laser fluence to produce samples and the size of nanoparticle grains calculated from XRD pattern

Samples	Sample 1	Sample 2	Sample 3	Sample 4
Laser fluence (J/cm^2)	0.3	0.6	0.9	1.2
Grain size ($2\theta = 33.7^\circ$) (nm)	3.99	7.69	11.89	13.89

height. Before ablation, Zn target was cleaned ultrasonically in acetone. The Zn target was irradiated vertically with the first harmonic of a Q-switched Nd:YAG laser ($\lambda = 1064$ nm) at 7 ns pulse width and 10 Hz repetition rate. Each sample was prepared with 5000 laser pulses. Samples 1–4 were prepared with laser pulse fluencies of 0.3, 0.6, 0.9, and 1.2 J/cm^2, respectively. Samples with some of their features are introduced in Table 1.

For calculating the ablated mass, Zn target was weighted before and after the ablation process. Sample 1 was almost colorless and the color of ZnO suspension was changed from bright brown to dark brown from sample 2–4 as is shown in Fig. 1.

Optical absorption spectra of samples in a 10 mm path length quartz cells were measured by UV–Vis-NIR spectrophotometer from PG Instruments (T-80). Crystalline structure of the samples was analyzed by X-ray diffraction (XRD) with Cu-Kα radiation ($\lambda =$ 1.54060 Å), using STOE-XRD diffractometer. The suspensions were dried on Si substrates XRD measurement. Also their morphology was studied by kyky EM3200 scanning electron microscopy (SEM) and Transmission Electron Microscopy (TEM, Philips EM 208). Room temperature photoluminescence (PL) of the samples was measured to characterize the luminescence properties of the nanoparticles. To investigate the molecular bonds in the suspensions the infrared spectroscopy FTIR, NEXUS 870 FT-IR system was used.

Results and Discussion

In Fig. 1, the photos of samples are presented, and in Fig. 2, the ablation mass of samples versus laser fluence is plotted. Depending on nanoparticle size and concentration, the color of ZnO nanoparticle solution in acetone can be varied from colorless to brown as is shown in Fig. 1. The color of sample 1 is light yellow which changes gradually to brown in sample

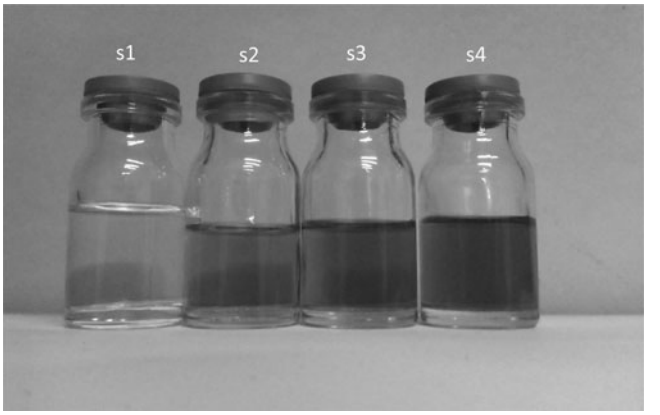

Figure 1. ZnO nanoparticle samples in acetone.

Downloaded by [University Town Library of Shenzhen] at 04:10 02 January 2016

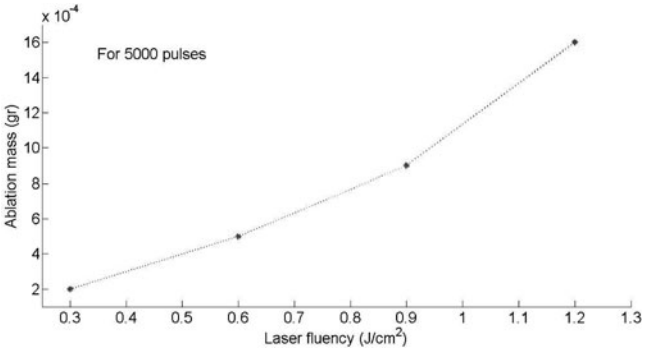

Figure 2. Variation of the mass of the target during the ablation versus laser pulse fluency.

4. Amount of nanoparticles in the acetone and size of produced nanoparticles are two reasons for changing the color of samples. In Fig. 2, it is shown that the amount of ZnO nanoparticles is increased exponentially with increasing the laser pulse fluence. In another experiment, the color of ZnO nanoparticles which were produced by laser ablation of Zn bulk in water was found the same [16].

XRD spectrums of nanoparticle as well as the X-ray diffraction pattern of the Zn target are presented in Fig. 3. In order to do this, measurement samples were dried on the silicon substrate at room temperature. The large peak at 69° is due to silicon substrate. The XRD spectrum clearly shows the crystalline structure of the nanoparticles and various peaks of zinc oxide (ZnO). We have the multi structure of nanoparticles that their peaks intensity is changed randomly for different samples. The XRD peaks of nanoparticles are very similar and most of them are different with Zn target peaks. It can be concluded that Zn and O atoms are composed randomly during the ablation process. Ablation of atoms has been taken place and nucleation has been occurred during the plasma plume expansion phase on the surface of target. The main dominant peaks can be identified at $2\theta = 31.8°$, 33.7°, 36.3°, 41.6°, 43.2°, 56.6°, and 82.1°. The XRD pattern of the ZnO nanoparticles in acetone at room temperature reveals that they are crystalline and possess the hexagonal wurtzite structure, however the wide peak at $2\theta = 33.7°$ is not indexed for the ZnO wurtzite structure

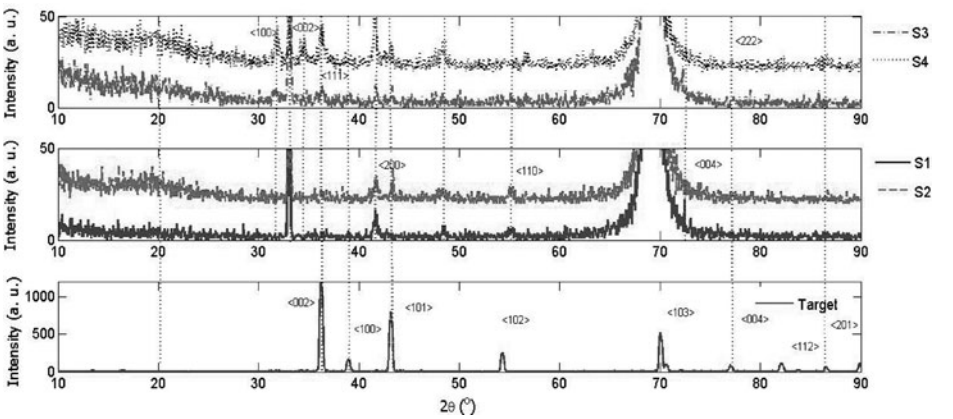

Figure 3. X-ray diffraction pattern of Zn target and dried ZnO nanoparticle samples.

Downloaded by [University Town Library of Shenzhen] at 04:10 02 January 2016

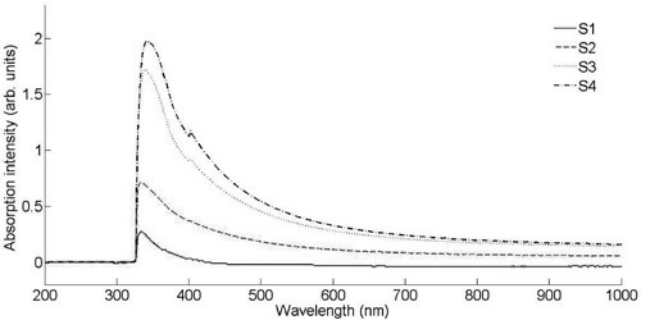

Figure 4. UV-Vis-NIR absorption spectrum of ZnO nanoparticles in acetone, with acetone as the reference.

Downloaded by [University Town Library of Shenzhen] at 04:10 02 January 2016

and is considered to steam from the ZnOOH nanoparticles [17]. The peaks at $2\theta = 36.3^\circ$ and 43.2° are due to hexagonal Zn structure which can be seen in the XRD pattern of target [18]. Results are in good agreement with other reports which are mostly on the production of ZnO nanoparticles by laser ablation in water [12–14, 17, 19–22].

The average grain size d of the nanoparticle of ZnO generated by laser ablation was estimated by using the standard Eq. (1) known as Scherrer formula [23]:

$$d = \frac{k\lambda}{\beta \cos\theta} \tag{1}$$

where k is a constant ($0.89 < k < 1$), λ is wavelength of the X-ray, β is the FWHM (Full Width at Half Maximum) of the diffraction peak, and θ is the diffraction angle. The mean grain size of nanoparticles are calculated using FWHM of peak at $2\theta = 33.7^\circ$, which is listed in Table 1. The grain sizes of nanoparticles are increased by increasing the laser fluence.

Absorption spectrums of nanoparticle solutions in the range of 200–1000 nm are presented in Fig. 4. The resonance absorption peak at 334–342 nm due to ZnO nanoparticles exciton resonance absorption can be observed. It can be seen that the intensity of absorption peaks and their FWHMs are different for samples. The most dramatic property of semiconductor nanoparticles is the size evolution of the optical absorption spectra. Hence UV-visible absorption spectroscopy is an efficient technique to monitor the optical properties of quantum-sized particles [24]. The influence of nanocrystal size on the electronic structure of semiconducting material is represented by the band gap increasing with decreasing of the particle size, which is attributed to the so-called quantum confinement

Table 2. Some characters of produced nanoparticles

Samples	Sample 1	Sample 2	Sample 3	Sample 4
Exciton absorption peak wavelength (nm)	334	334	338	342
Absorption intensity	0.28	0.717	1.722	1.984
Bandgap energy (eV)	3.37	3.33	3.33	3.30
Transmission	0.005	0.0055	0.0055	0.0025
Photoluminescence peak (nm)	375	377	378	379

effect. If the size of nanoparticles increases, their resonance absorption spectrum peak will be shifted toward larger wavelength and vise-versa. For exciton resonance phenomenon to happen, the particle must be much smaller than the wavelength of incident light. A red shift in the absorption spectrum is due to increasing the average nanoparticle size in samples, that the absorption measurements provide a qualitative indication of the crystal size distribution. The sharp excitonic peak in the absorption spectra in the case of small nanocrystals (at higher laser pulse energy) is indeed indicative of the narrow size distribution of the nanoparticles in the samples. For the larger particles, sharp excitionic features are not present in the absorption spectra (at lower laser pulse energy). This is due to the fact that a number of exciton peaks appear at different energies corresponding to different sized nanocrystals which overlap with each other. Therefore, a broadened size distribution of the nanocrystals can be expected. This assumption is confirmed by the number size distributions recorded by using other diagnostics. The intensity of the absorption peaks of samples as well as their FWHMs and their corresponding wavelengths are presented in Table 2. The intensity of excitonic absorption peak is increased with increasing the laser pulse energy during the ablation process, which can be due to increasing the concentration of nanoparticles in the suspensions. A red shift in the wavelengths at which peaks are occurred can be observed. According to Mie theory, this red shift confirms an increase in the size of produced nanoparticles from sample 1–4. Appearance of one peak in the spectrum shows that the width of the size distribution function of produced nanoparticles in suspensions is narrow.

Downloaded by [University Town Library of Shenzhen] at 04:10 02 January 2016

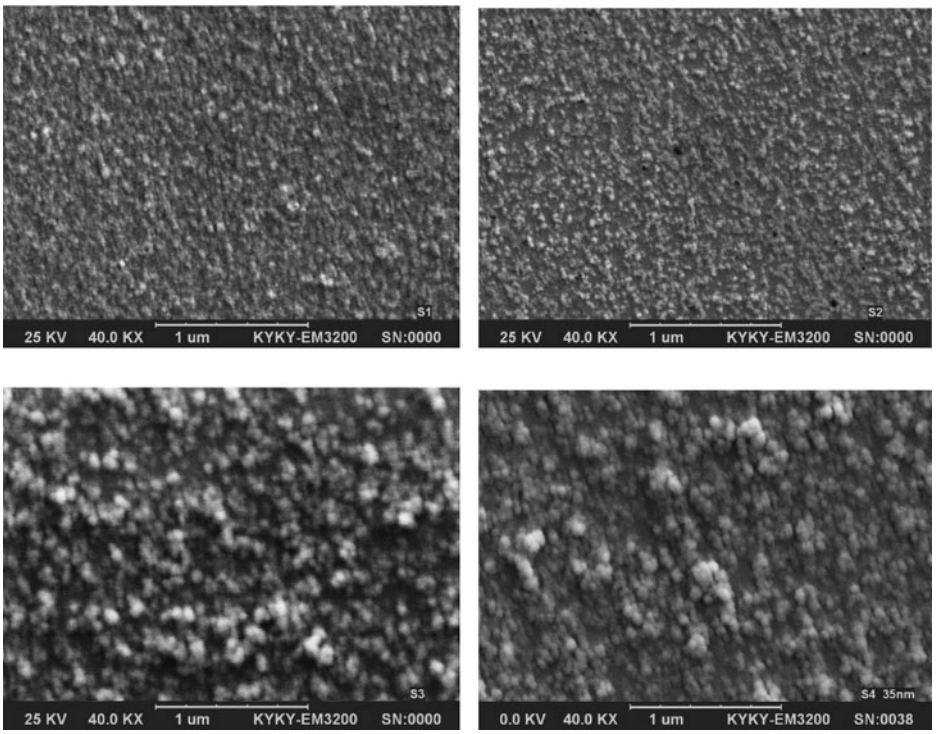

Figure 5. SEM micrographs of ZnO nanoparticles samples dried on aluminum foil.

Downloaded by [University Town Library of Shenzhen] at 04:10 02 January 2016

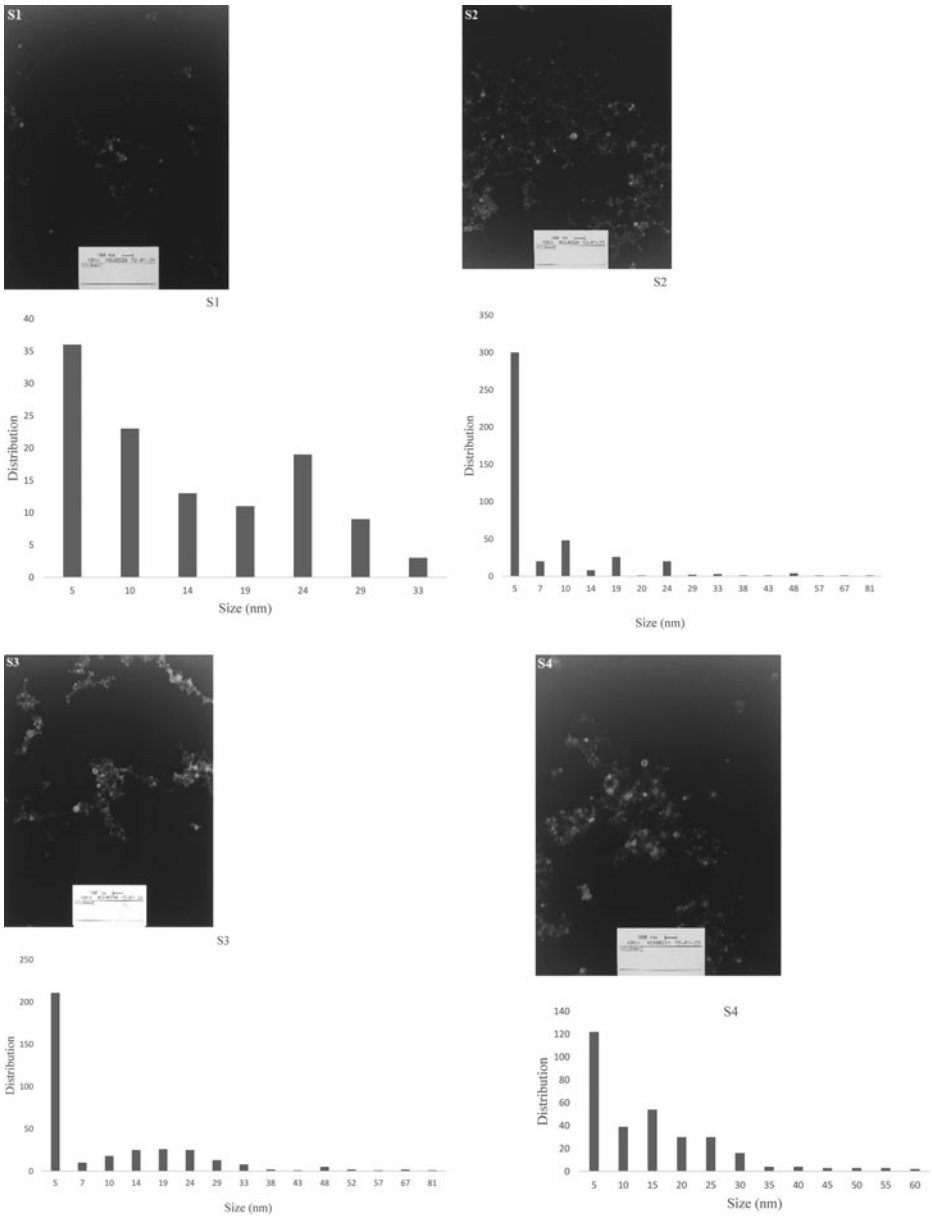

Figure 6. TEM image and size distribution of ZnO nanoparticle generated in acetone with laser ablation method.

Figure 5 presents SEM images of ZnO nanoparticles prepared by laser ablation in acetone. Images are taken using 25 keV electrons leads to 40 kX magnification. Morphology of ZnO nanoparticles depends on laser pulse energy and also is influenced by laser pulse wavelength and ablation environment. As can be seen, the density of ZnO nanoparticles in acetone is increased with increasing the fluence of the laser pulse. The particles are almost spherical and adhered to each other. The morphology of nanoparticles is strongly depends

on the ablation environment in the experiment. The ZnO nanoparticles prepared by laser pulse of 1064 nm wavelength in water are reported to be sheet-like and spherical [16]. The ZnO nanoparticles prepared by laser pulse of 1064 nm wavelength in other environments such as CTAB are reported to be spindle like [14]. In the case of acetone as the ablation environment particles are all spherical. In this result, the effect of higher energy particles can be observed. With increasing the laser fluence, adhesion of particles is decreased. Effect of laser pulse energy on the size of produced nanoparticles is clear in Fig. 5. From sample 1–4, the number of larger particles in the SEM micro images is increased.

TEM images of the nanoparticles on the scale of 100 nm are displayed in Fig. 6. The smallest nanoparticle in samples can be seen in these images. Size distribution functions of particles are plotted with their TEM images. The peak of size distribution of ZnO nanoparticles produced in acetone is at 5 nm. This size range is more smaller than that reported on producing ZnO nanoparticles in similar experimental condition in other environments [14, 25]. The products are composed of particles with nearly spherical shape, similar to other reports [26]. With increasing the laser fluence, the concentration of nanoparticles in solutions is increased. Number of large particles in samples is increased from sample 1 to 4. In other words the average size of ZnO nanoparticles is increased with increasing the laser fluence in the ablation process. This variation is in good agreement with the red shift which was occurred in the excitonic peak of absorption spectrum of samples.

From transmission spectrum of samples, their bandgap energy is calculated. To calculate the absorption band edge of the samples, the first derivative of the optical transmittance can be computed using MATLAB software. The peak of $dT/d\lambda$ curve occurs at the wavelength corresponds to bandgap energy of samples, which are presented in Table 2. Bandgap transition wavelength of samples are in the range of 368–376 nm, correspond to photon energy in the range of 3.29–3.36 eV. Similar results are reported in other researches [13, 23]. From sample 1–4 with increasing the laser fluence during the synthesize process, the bandgap energy of nanoparticles is decreased. It can be due to increasing the number of atoms, i.e., defect levels, in the structure of nanoparticles. With increasing the size of nanoparticles their bandgap energy is expected to decrease. This result is in very good agreement with red shift of excitonic peak and SEM and TEM images.

A study of the PL property of any material is interesting because it can provide valuable information on the quality and purity of the material. The semiconductor ZnO nanoparticles,

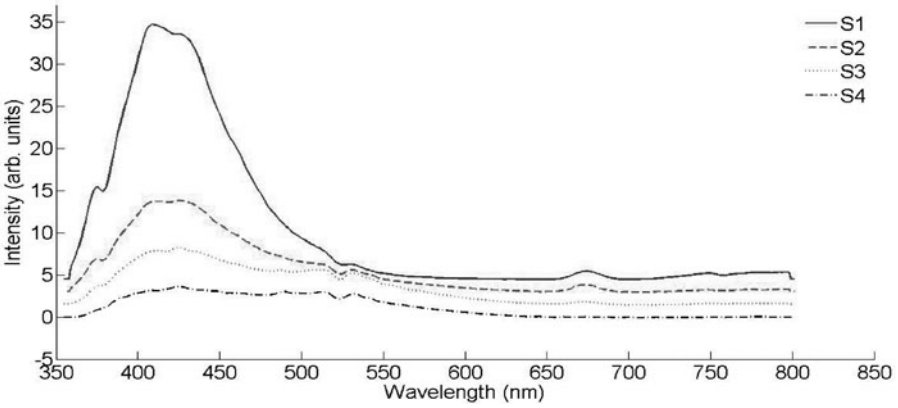

Figure 7. Photoluminescence spectrum of ZnO nanoparticles in acetone.

Downloaded by [University Town Library of Shenzhen] at 04:10 02 January 2016

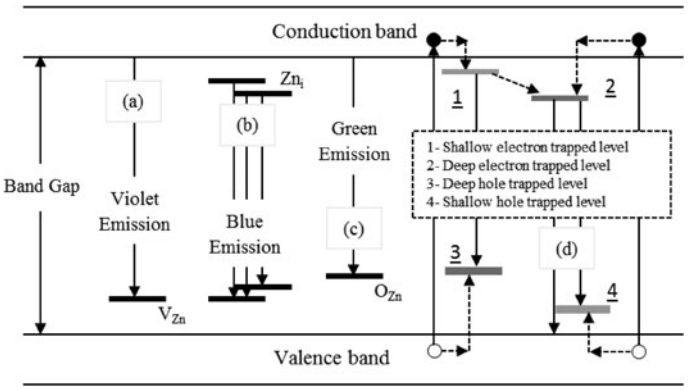

Figure 8. Schematic view of the energy band diagram proposed for ZnO nanoparticle.

with sizes comparable to or below their exciton Bohr radius, have distinctive electronic and optical behaviors due to exciton quantum confinement phenomena. For such reasons, "quantum dots" suitably describes these semiconductor nanoparticles which absorb light at specific wavelength and emit it at longer ones. Therefore, recording of PL spectrum is of paramount importance for estimating the size of nanoparticles and their characteristics for various applications [27]. In the photoluminescence spectra of ZnO, typically there are emission bands in the UV and visible regions. The UV peak is usually considered as the characteristic emission of ZnO and attributed to the bandedge emission or the exciton transition [28], while the emission bands in the visible range are due to the recombination of photo-generated holes with singly ionized charge states in intrinsic defects such as

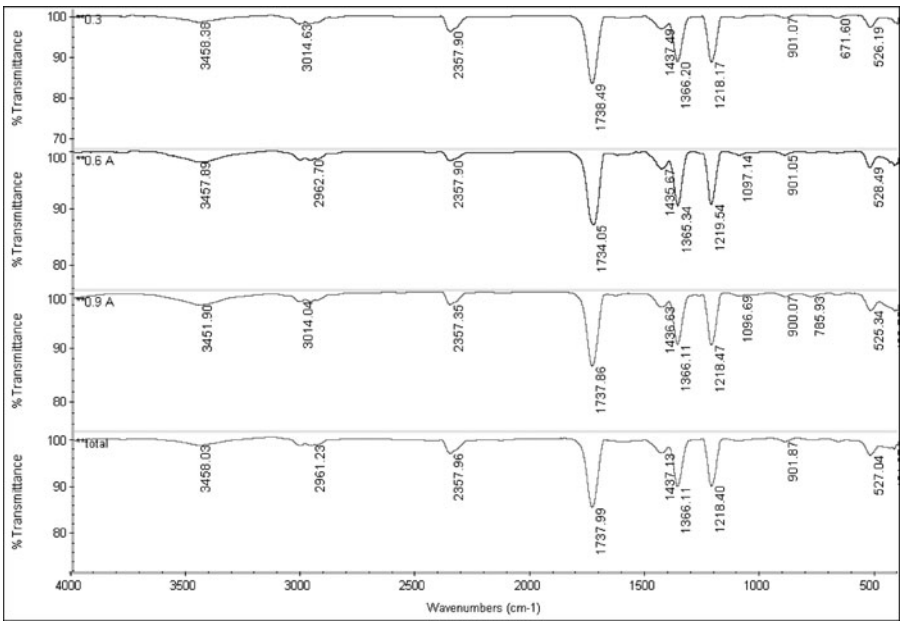

Figure 9. IR transmission spectrum of samples.

Downloaded by [University Town Library of Shenzhen] at 04:10 02 January 2016

oxygen vacancies, Zn interstitials, or impurities [29]. Generally, the UV emission in ZnO disappears in two cases. First, if the excitation energy is considerably lower that its band gap energy and second, if the intensity of visible emission is much higher due to increased defect density [28].

Figure 7 shows the room temperature photoluminescence spectra from ZnO nanoparticles on irradiating at excitation wavelength 335 nm by a xenon lamp. Spectra exhibit two main emissions. One UV emission band in the range of 375–379 nm and one visible wide emission band in the range of 410–430 nm, which are presented in Table 2. The peak at 375–379 nm can be attributed to the interband transition from conduction band to valance band. The magnitude of wavelength correspond to this peak is very close to calculated bandgap wavelength. The next peaks in the range of 410–430 nm are due to defect levels as mentioned.

The PL intensity of UV emission is increased with increasing the laser pulse energy form 0.75–1.5 J, while the intensity of visible emission is decreased. On the other words, the sharp excitonic emission indicates that the ZnO nanostructure have a low defect concentration and relevant optical properties [30]. The same red shift can be observed in the PL spectra of samples which are occurred in both main peaks, shows that PL peaks are very sensitive to the size of nanoparticles.

Based on the observed PL results, the schematic energy level diagram of ZnO nanoparticles can be depicted as shown in Fig. 8. The presence of different types of defects and their effect are considered in this model. The first principle study shows that the Zn_{3d} electron strongly interacts with the O_{2p} electron in ZnO. Oxygen has tightly bound 2p electrons and Zn has tightly bound 3d electrons, which sense the nuclear attraction efficiently. Violet luminescence is attributed to the transition from conduction band to the deep holes trapped levels like V_{Zn} as is shown in the Fig. 8a. The blue emission can be ascribed to the direct recombination of conduction electron in the Zn_{3d}band and a hole in the O_{2p} valance band. Figure 8d shows the typical process for green emission: the mechanism of the transition (1) from near conduction band edge to deep acceptor level and (2) from deep donor level to valence band. The recombination of shallowly trapped electron with a deeply trapped hole in $V_o{}^{++}$ center causes visible emission [28].

FTIR spectrum was recorded in the spectral range of 400–4000 cm^{-1}. The FTIR spectra of ZnO nanoparticles prepared by laser pulse with different energy in acetone are shown in Figs. 9 and 10. In comparison with other reports several peaks are appeared in the FTIR spectrum of nanoparticles solution when ablation is carried out in acetone [10, 12]. These

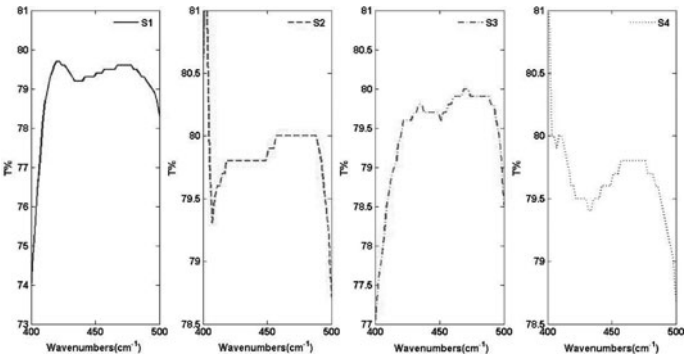

Figure 10. IR transmission spectrum of ZnO nanoparticles in 400–500 (cm^{-1}) range.

Downloaded by [University Town Library of Shenzhen] at 04:10 02 January 2016

impurities such as OH and CO absorb by ZnO nanoparticles during the FTIR measurement. The absorption peak in the range of 3451–3459 cm^{-1} are correlated to the acetone O−H stretching vibration. In the spectrum of samples 1 and 2 we observed two picks in 6229 and 2961 cm^{-1} due to CH_3. The absorption peak revealing the vibrational properties of ZnO nanoparticles is observed at 410–500 cm^{-1} as can be seen in Fig. 10. The absorption peaks of OH bending and C=O due to ZnO nanoparticles almost are in the same range of transmittance [25].

Conclusion

In conclusion, ZnO nanoparticles were prepared by pulse laser ablation method in acetone as a liquid environment, because of its potential to decreases the size and the aggregation of NPs. In this work, the effects of laser pulse energy and liquid environment on the nanostructure, morphology, optical properties of ZnO nanoparticles have been investigated. XRD data reveal that these nanoparticles possessed the hexagonal wurtzite structure. Red shift in absorption spectrum of ZnO nanoparticles and TEM images showed that the size distribution and particle size of ZnO nanoparticles is increased with increasing laser fluence. Also PL spectrum authenticates this issue. PL result is in good agreement with the calculated bandgaps. SEM image indicate that the morphology of ZnO nanoparticles was spherical. FTIR transmittance spectra of ZnO nanoparticles proved the existence of characteristic peak of ZnO at 410–500 cm^{-1}.

References

[1] Noel, S., Hermann, J., & Itina, T. (2007). *Appl. Surf. Sci.*, *253*, 6310–6315.
[2] Solati, E., Mashayekh, M., & Dorranian D., (2013). *Appl Phys A*, *112*, 689–694.
[3] Abdolmaleki, A., Mallakpourb, S., & Borandeh, S., (2011). *Appl. Surf. Sci.*, *257*, 6725–6733.
[4] Huang, M. H., Mao, S., Feick, H., Yan, H. Q., Wu, Y. Y., *et al.* (2001). *Science*, *292*, 1897–1899.
[5] Mo, C. M., Li, Y. H., Liu, Y. S., Zhang, Y., & Zhang, L. D. (1998). *J. Appl. Phys.*, *83*, 4389–4391.
[6] Mote, V. D., Purushotham, Y., & Dole, B. N. (2012). *J. Theo. Appl. Phys.*, *6*, 1–8.
[7] Djurisic, A. B., Ng, A. M. C., & Chen, X. Y. (2010). *Prog. Quant. Electron.*, *34*, 191–259.
[8] He, C., Sasaki, T., Shimizu, Y., & Koshizaki, N. (2008). *Appl. Surf. Sci.*, *254*, 2196–2202.
[9] Li, B., Kawakami, T., & Hiramatsu, M., (2003). *Appl. Surf. Sci.*, *210*, 171–176.
[10] Gondal, M. A., Drmosh, Q. A., Yamani, Z. H., & Saleh, T. A. (2009). *Appl. Surf. Sci.*, *256*, 298–304.
[11] Ishikawa, Y., Shimizu, Y., Sasaki, T., & Koshizaki, N., (2006). *J. Colloid Interf. Sci.*, *300*, 612–615.
[12] Drmosh, Q. A., Gondal, M. A., Yamani, Z. H., & Saleh, T. A., (2010). *Appl. Surf. Sci.*, *256*, 4661–4666.
[13] He, C., Sasaki, T., Usui, H., Shimizu, Y., & Koshizaki, N. (2007). *J. Photochem. Photobiol., A 191*, 66–73.
[14] He, C., Sasaki, T., Shimizu, Y., & Koshizaki, N. (2008). *Appl. Surf. Sci*., *254*, 2196–2202.
[15] Faramarzi, S., Jalilian-Nosrati, M. R., & Barcikowski, S. (2010). *J. Theo. Appl. Phys.*, *4*(1), 6–9.
[16] Solati, E., Dejam, L., & Dorranian, D. (2014). *Opt. Laser Technol.*, *58*, 26–32.
[17] Cho, J. M., Song, J. K., & Park, S. M., (2009). *Bull. Korean Chem. Soc.*, *30*, 1616–1618.
[18] Zeng, H., Cai, W., Li, Y., Hu, J., & Liu, P., (2005). *J. Phys. Chem. B*, *109*, 18260–18266.
[19] Van Hieu, N., & Duc Chien, N., (2008). *Physica B*, *403*, 50–56.
[20] Abdolmaleki, A., Mallakpour, Sh., & Borandeh, S., (2011). *Appl. Surf. Sci.*, *257*, 6725–6733.
[21] Ishikawa, Y., Shimizu, Y., Sasaki, T., & Koshizaki, N., *J. Colloid Interface Sci.*, *300*, 612–615.
[22] Thareja, R. K., & Shukla, S. (2007). *Appl. Surf. Sci.*, *253*, 8889–8895.

Downloaded by [University Town Library of Shenzhen] at 04:10 02 January 2016

[23] Suryanarayana, C., & Norton, M. G., (1998). *X-Ray Diffraction a Practical Approach*, Plenum Press: New York.
[24] Srinivasa Rao, B., Rajesh Kumar, B., Rajagopal Reddy, V., Subba Rao, T., & Venkata Chalapathi, G. (2011). *Chalcogenide Lett.*, *8*, 39–44.
[25] Dorranian, D., Solati, E., & Dejam, L. (2012). *Appl. Phys. A*, *109*, 307–314.
[26] Zeng, H., Cai, W., Li, Y., Hu, J., & Liu, P. (2005). *J. Phys. Chem. B*, *109*, 18260–18266.
[27] Gondal, M. A., Drmosh, Q. A., Yamani, Z. H., & Saleh, T. A. (2009). *Appl. Surf. Sci.*, *256*, 298–304.
[28] Kundu, T. K., Karak, N., Barik, P., & Saha, S. (2011). *Int. J. Soft Comput. Eng.*, *1*, 19–24.
[29] Kenanakis, G., Androulidaki, M., Koudoumas, E., Savvakis, C., & Katsarakis, N. (2007). *Superlattices Microstruct.*, *42*, 473–478.
[30] Xu, F., Yuan, Z. Y., Du, G. H., Ren, T. Z., Bouvy, C., *et al.* (2006). *Nanotechnology*, *17*, 588–594.

Downloaded by [University Town Library of Shenzhen] at 04:10 02 January 2016